

Nanostructured Polymer Gels

Zhibing Hu

Departments of Physics and Chemistry, University of North Texas
P. O. Box 311427, Denton, TX 76203, USA

Summary: A brief review of our recent work on polymer gel opals is given in memory of late Professor Tanaka. The central idea is to first synthesize monodisperse polymer gel nanoparticles, then self-assemble them into a 3D network, and eventually covalently bond them. The covalent bonding contributes to the structural stability, while self-assembly provides them with crystal structures that diffract light, resulting in colors. N-isopropylacrylamide (NIPA) gel has been used as a model system for this study. The nanostructured NIPA gel, which contain up to 97 wt % water, displays a striking iridescence like precious opal but are soft and flexible like gelatin.

Introduction

With his unique story-telling style, late Professor Tanaka has shown us that polymer gels can swell or collapse reversibly in response to external stimuli.^[1-3] His pioneering research not only opened a door for fundamental scientific study^[4-7] and practical applications^[8-14] but also inspired a new generation of polymer scientists. Here a brief review of our recent work^[15-17] on nano-structured polymer gels is given in memory of late Professor Tanaka.

Polymer gels are a class of macromolecular networks that contain a large fraction of solvent such as water within their structure.^[18] Polymer gels are usually formed by the free radical polymerization of monomers in the presence of a difunctional crosslinking agent and a solvent. They can be made either in bulk or in nano- or micro-particles. The bulk gels are easy to handle, but usually have very slow swelling rate and amorphous structures arising from randomly crosslinked polymer chains, while the gel nanoparticles react quickly to an external stimulus, but are too small for some practical applications. Recently, creating nanostructures in gels has attracted attentions. Such structures include gels with embedded self-assembled solid polymer spheres^[19-20] and the complex formation of polyelectrolyte gels with oppositely charge surfactants.^[21]

We have proposed to synthesize bulk gels by covalently bonding self-assembled gel nanoparticles (also called colloidal gel particles or microgels).^[15-16] The covalent

bonding contributes to the structural stability, while self-assembly provides them with crystal structures that diffract light, resulting in colors. Such stable periodic 3D structures allow us to obtain useful functionality not only from the constituent gel building blocks but also from the long-range ordering that characterizes these structures.

A nanostructured polymer gel should have a two-level structural hierarchy as shown in Figure 1 (left panel): The primary network (I) consists of crosslinked polymer chains inside each nanoparticle, while the secondary network (II) is a crosslinked system of the nanoparticles. The mesh sizes of the primary and the secondary networks are typically around 1-10 nm and 10-500 nm respectively. The networks could have randomly packed structure (left panel, Fig. 1) or periodic structures (right panel, Fig. 1).

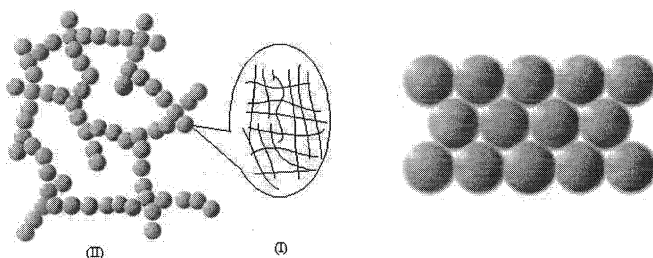


Figure. 1. Conceptual models. Left panel: The model of the two-level structural hierarchy for all gel nanoparticle networks: the primary network (I) consists of crosslinked polymer chains inside each nanoparticle, while the secondary network (II) is a system of the crosslinked nanoparticles. Right panel: The networks could have periodic structures.

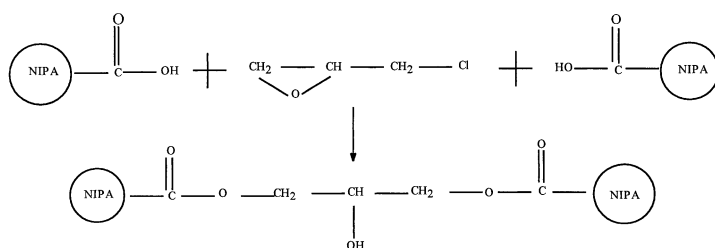
We have chosen N-isopropylacrylamide (NIPA) gel as a model system for this study. Since Tanaka and co-workers' pioneering work,^[3] the NIPA gel has been extensively studied in various structural forms including macrogel,^[4-5, 11] porous gel,^[12] and microgels.^[22-25]

Experimental

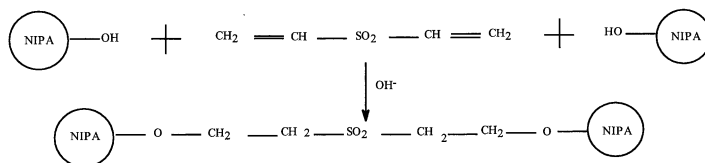
N-isopropylacrylamide (NIPA) nanoparticles and two of its derivatives, with various particle sizes, were synthesized using an emulsion polymerization method.^[22] One derivative was NIPA co-polymerized with acrylic acid (AA) and the other was NIPA co-polymerized with 2-hydroxyethyl acrylate (HEAc). The NIPA had thermally responsive properties,^[3] while the AA and the HEAc provided carboxyl (-COOH) and

hydroxyl (-OH) groups, respectively, for the crosslinking sites. The pure NIPA nanoparticles were used as a model system for the study of colloidal crystallization and the NIPA derivative nanoparticles were used as building blocks for synthesis of nanoparticle networks. The size distribution of nanoparticles was characterized using a light scattering spectrometer (ALV-5000). The hydrodynamic radius of the resultant nanoparticles in water was narrowly distributed with a size variance of about 1%.

Scheme 1



Scheme 2



We have developed two schemes for covalently bonding nanoparticle assemblies in either organic or aqueous media. In the first scheme, the NIPA-AA nanoparticles in water were first precipitated by adding acetone. These concentrated nanoparticles were transferred to a mixture of acetone/epichlorohydrin (1:3 volume ratio) to form a short-range-ordered structure by steric and electrostatic repulsion. After incubation at 98 °C for 10 h, the nanoparticles formed a three-dimensional network. This network was immersed in acetone and finally in de-ionized water for thorough washing. In the second scheme, the NIPA-HEAc nanoparticles first self-assembled into different structural arrays at various concentrations in an aqueous solution (pH=12). Then, divinylsulfone (DVS) ^[12] was added to bond them at room temperature. The second scheme can be carried out directly in water and is particularly useful for hydrogels. Since the colloidal particles are linked together by covalent bonding, they cannot be re-dispersed into a solution, in contrast to well-known colloidal aggregates. It is noted that the crosslinkers can react not only with the functional groups of different nanoparticles

but also with those of the same particles. It will be an interesting study to find the ratio of intra- versus inter-particle crosslinking.

Results and Discussion

Characterization of NIPA nanoparticles. Figure 1 shows a typical hydrodynamic radius distribution of NIPA nanoparticles in dilute dispersions at 25 and 40 °C respectively, where dynamic light scattering measurements were done at an angle of 20 degrees.^[17] At temperatures lower than the phase transition temperature ($T_c \sim 34$ °C), the microgels are in their swelling state and are narrowly distributed. The average hydrodynamic radius ($\langle R_h \rangle$) at 25 °C is 132 nm. At 40 °C, the nanoparticles shrink sharply ($\langle R_h \rangle = 49.8$ nm with a narrower size distribution) but are fully dispersed.

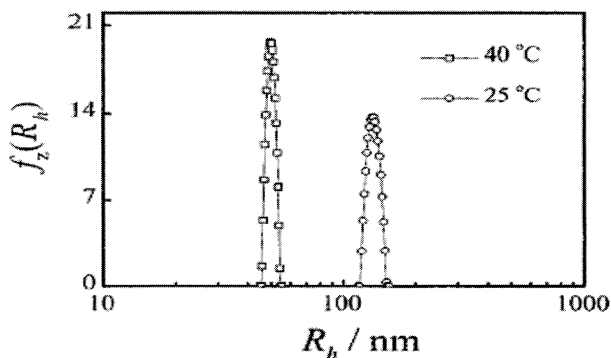


Figure 2. Hydrodynamic radius distributions ($f(R_h)$) of NIPA nanoparticle spheres in water at $T = 25.0$ °C (circles) and 40.0 °C (squares), respectively, where $C = 1.37 \times 10^{-5}$ g/g, and the scattering angle is 20° .^[17]

Self-assembling of NIPA nanoparticles in water. As the concentration of NIPA nanoparticle dispersion increases at room temperature (18 to 22 °C, below T_c), all spheres can be close-packed, resulting in remarkable change in rheological and optical properties. From light scattering, optical and turbidity measurements, a schematic “phase diagram” is constructed for a very broad distribution of polymer concentrations ranging from 0.01 to 14 wt % as shown in Fig. 3. The assemblies exhibit different structures as the polymer concentration changes: the *liquid* phase (Fig. 3. (A-C)) where spheres are free to move around; the *crystal* phase (D-E) where the freedom of the

spheres is limited and the particles can self-assemble into a long-range ordered state, and the *glass* phase (F-I) where the movement of the spheres is highly limited.

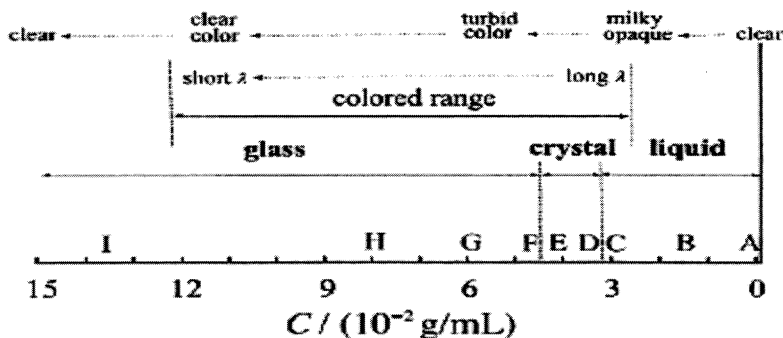


Figure 3. Schematic "phase diagram" of the NIPA colloidal water dispersions as a function of polymer concentration C (wt%).^[17] The average hydrodynamic radius of NIPA spheres in water at 25 °C is 132 nm.

The corresponding optical appearance changes first from clear to opaque in dilute dispersion, then to pink, green, blue and blue-violet color in the concentrated dispersions, and eventually to transparent in highly concentrated dispersion. The

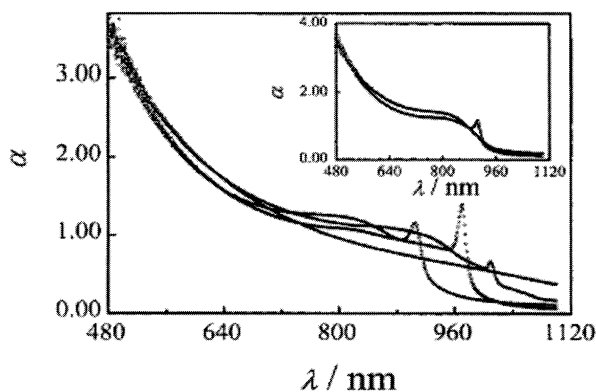


Figure 4. The turbidity is plotted as a function of wavelength for NIPA microgel dispersions at various C , where the average hydrodynamic radius of NIPA microgel spheres in dilute water dispersions at 25 °C is 216 nm.^[17] The curves with a peak from left to right correspond to $C=4.47 \times 10^{-2}$, 3.65×10^{-2} , and 3.21×10^{-2} g/g, respectively. The curve without a peak corresponds to $C=1.99 \times 10^{-2}$ g/g. The inset compares the turbidity curves before (with a peak) and after shear melting (without a peak) for the sample of $C=4.47 \times 10^{-2}$ g/g.

formation of crystals around a concentration of about 3 ~5 wt % adds iridescent patterns to the background colors.

The optical appearance of the NIPA nanoparticle dispersions can be better revealed by turbidity measurements as shown in Figure 4 for polymer concentration between ~ 3 and ~ 5 wt%. Here NIPA microgel spheres have not only strong interaction but also enough freedom to form large colloidal crystals at room temperature. These crystals are easy to observe due to their iridescent patterns. The turbidity exhibits either a sharp peak or a sudden increase with decrease of wavelength, as shown in Figure 4. The iridescent patterns originate from Bragg diffraction. Constructive interference occurs if Bragg condition: $2nds\sin\theta = m\lambda$, is satisfied, where d , θ , n , λ , m are the lattice spacing, the diffraction angle, the refractive index of the gel medium, the wavelength of light in vacuum and an integer, respectively. These crystals are not strong and can be easily destroyed by shaking the dispersion as shown in the inset of Figure 4, where turbidity curves are compared before and immediately after shear melting of the crystals.

We consider that the color of the dispersions originates from interference that relates to the ordered inter-particle distance. Let us define λ_c as the transition wavelength corresponding to the peak or the middle height of the shoulder in the turbidity curve. From Figure 4 and other measurements (not listed), λ_c as a function of polymer concentration was measured and shown in Figure 5. Here, we have converted the

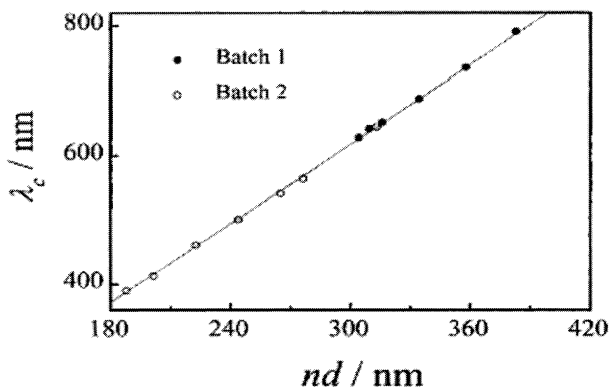


Figure 5. Influence of the inter-particle light distance nd on λ_c , at which the turbidity exhibits a peak or a shoulder-shape increase with the decrease of wavelength.^[17] Two Batches of samples are combined together: Batch 1 (solid circles), $R_h = 132$ nm and Batch 2 (open circles), $R_h = 216$ nm at 25 °C. The line represents the least square fitting of λ_c (nm) = $2.04nd + 4.1$ where n is the refractive index of the microgel.

concentration of the samples into the inter-particle distances by considering that the microgel spheres form face-centered cubic structured as revealed by small angle neutron scattering.^[26] The increase in weight fraction of microgel spheres reduces the inter-particle distance so that λ_c shifts to a lower wavelength. Because of suitable size range of our samples, λ_c can be tuned to cover whole visible light wavelength range. It is also noted that λ_c is larger for dispersions with the same weight fraction but larger particle size.

The least square linear fit of λ_c with inter-particle optical path length (nd) in Figure 5 leads to the relation: $\lambda_c(\text{nm}) = 2.04nd + 4.1$. Here we have taken into account of the refractive index (n) change with the weight fraction of microgel spheres using weight additive method, $n = 1.6C + 1.33(1-C)$, where 1.6 and 1.33 are refractive indexes of PNIPA and water respectively, and C is the concentration. λ_c well satisfies the Bragg diffraction condition of $2nds\sin\theta = m\lambda_c$ at $\theta = 90^\circ$ and $m = 1$.

The properties of NIPA nanoparticle networks. The covalent linkages between nanoparticles lead to the remarkable thermal stability of the crystal structure. Figure 6 shows the temperature dependence of a crystal hydrogel in a tube after polymerization with Scheme 2. The iridescent pattern (left panel) at room temperature became invisible when the sample was heated to 50 °C, at which point the gel became cloudy due to phase separation (right panel). When the sample at 50 °C was cooled back to 21 °C, the pattern reappeared within 10 s, and this process was reversible.

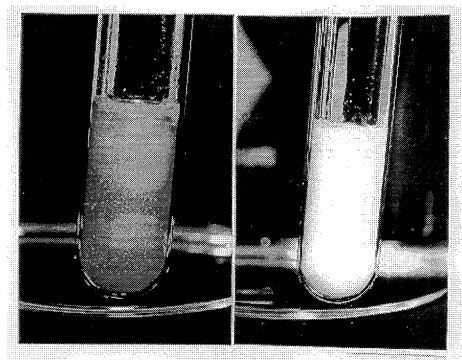


Figure 6. The NIPA crystal hydrogels made according to Scheme 2.^[16] The sample in the tube is transparent and exhibited an iridescent pattern at 21 °C (left) until the temperature was raised to 50 °C (right), at which point the pattern became invisible. As the sample at 50 °C was cooled back to 21 °C, the patterns reappeared within 10 s.

In contrast, a non-crosslinked nanoparticle assembly with the same concentration was completely disrupted as the temperature was raised to 30 °C. It required about 1000 times longer for a non-crosslinked assembly to re-assemble into a crystal structure. It is apparent that disturbed nanoparticles in a crosslinked assembly are able to return to their equilibrium crystalline positions quickly through restoring forces provided by the network elasticity. The fast response rate of the crystal hydrogels could be a major advantage for developing sensor or display technologies over conventional colloidal crystal arrays.

It is noted from the left panel in Figure 6 that the crystal hydrogel in water displays an iridescent color with good transparency and no sedimentation (without adding an index-matching or a density-matching fluid). This is because the building blocks are hydrogel nanoparticles that contain up to 97 wt% water; both the refractive index and the density of the particles are nearly matched with those of the surrounding water.

Conclusion

Along the avenue paved by the late Professor Tanaka and coworkers on NIPA gels, we have synthesized NIPA gel opals by covalently bonding self-assembled gel nanoparticles. The major steps consist of (1) synthesizing monodisperse polymer gel nanoparticles, (2) self-assembling them into a 3D network, and (3) covalently bonding these particles. Covalent bonding contributes to the mechanical and thermal stability of the assemblies, while self-assembly provides the bulk hydrogels with crystal structures which diffract light, resulting in colors. The polymer nanoparticle networks could be used as a directly observable (in 3D real space) model system to study a wide variety of fundamental phenomena such as crystallization, phase transition, and fracture mechanics. Creating such nanostructured materials is also of importance in technological applications including controlled drug delivery, biomaterials, sensors, devices, bio-adhesives, and displays.

Acknowledgment This work is supported by the National Science Foundation under Grant No. DMR-0102468, the U.S. Army Research Office under Grant No. DAAD 19-01-1-0596. I thank Drs. J. Gao and X. H. Lu for their contributions to this project.

- [1] T. Tanaka, *Phys. Rev. Lett.* **1978**, 40, 820.
- [2] T. Tanaka, I. Nishio, S. T. Sun, S. Ueno-Nishio, *Science* **1982**, 218, 467.
- [3] S. Hirotsu, Y. Hirokawa, T. Tanaka, *J. Chem. Phys.* **1987**, 87, 1392.
- [4] M. Shibayama, T. Tanaka and C. C. Han, *J. Chem. Phys.* **1992**, 97, 6829; *J. Chem. Phys.* **1992**, 97, 6842.
- [5] G. Liao, Y. Xie, K. F. Ludwig, R. Bansil, and P. Gallagher, *Phys. Rev. E* **1999**, 60, 4473.
- [6] Y.L. Yin and F. Stanley and R.K. Prud'homme, In *Polyelectrolyte Gels*, R. Harland and R.K. Prud'homme, eds., ACS Symposium Series, **1992**, 480.
- [7] J.P. Baker, H.W. Blanch and J.M. Prausnitz, *Polymer* **1995**, 36, 1061.
- [8] R. A. Siegel, B. A. Firestone, *Macromolecules* **1988**, 21, 3254.
- [9] Y. Osada, H. Okuzaki, H. Hori, *Nature* **1992**, 355, 242.
- [10] G. Chen, A. S. Hoffman, *Nature* **1995**, 373, 49.
- [11] Y. Osada, and J. P. Gong, *Adv. Mater.* **1998**, 10, 827.
- [12] D. C. Harsh, S. H. Gehrke, *J. Controlled Release* **1991**, 17, 175.
- [13] Z. Hu, X. Zhang, Y. Li, *Science* **1995**, 269, 525.
- [14] M. J. Snowden, M. J. Murray and B. Z. Chowdry, *Chemistry & Industry* **1996**, 531.
- [15] Z. Hu, X. Lu, J. Gao, and C. Wang, *Advanced Materials* **2000**, 12, 1173.
- [16] Z. Hu, X. Lu and J. Gao, *Advanced Materials* **2001**, 13, 1708.
- [17] J. Gao and Z. Hu, *Langmuir* **2002**, 18, 1360
- [18] A. S. Hoffman, *J. Control. Release* 6, 297 (1987).
- [19] J. M. Weissman, H. B. Sunkara, A. S. Tse, S. A. Asher, *Science* **1996**, 274, 959 .
- [20] J. H. Holtz, S. A. Asher, *Nature* **1997**, 389, 829.
- [21] E. Sokolov, F. Yeh, A. R. Khokhlov, V. Y. Grosberg and B. Chu, *J. Phys. Chem. B* **1998**, 102, 7091.
- [22] R. H. Pelton, P. Chibante, *Colloids and Surfaces* **1986**, 20, 247.
- [23] C. Wu and S. Zhou, *Macromolecules* **1996**, 29, 1584.
- [24] H. Senff, W. Richtering, *J. Chem. Phys.* **1999**, 111, 1705.
- [25] J. D. Debord and L. A. Lyon, *J. Phys. Chem.* **2000**, 104, 6327.
- [26] T. Hellweg, C.D. Dewhurst, E. Bruckner, K. Kratz, and W. Eimer, *Colloid Polym. Sci.* **2000**, 278, 972.

